Conference - ISSS-6 -

Chemical Vapor Deposition of Hexagonal Boron Nitride*

Satoru Suzuki[†] and Hiroki Hibino

NTT Basic Research Laboratories, NTT Corporation,
3-1, Morinosato Wakamiya, Atsugi, Kanagawa 243-0198, Japan

Nanometer-thick hexagonal boron nitride thin films were grown by thermal chemical vapor deposition on polycrystalline Ni, Co, and Cu substrates. A thicker and more regularly stacked film was grown on a Ni substrate, whereas a smaller film thickness and more turbostratic stacking or smaller domain size were observed on Cu. Intermediate situations were observed on Co. The substrate material dependence strongly suggests that the substrate plays an important role in h-BN growth, like it does in graphene growth, although nitrogen is almost insoluble even in Ni. Grain boundaries may accommodate boron and nitrogen atoms at a growth temperature. [DOI: 10.1380/ejssnt.2012.133]

I. INTRODUCTION

Hexagonal boron nitride (h-BN) is a structural analog of graphene with an ideally small lattice mismatch (2 %). In remarkable contrast to the fact that graphene has no band gap, h-BN has a large band gap (~ 6 eV [1]) because of a certain degree of ionic character of the B-N bond. Thus, h-BN is often called "white graphene" recently [2,3]. Combining graphene and h-BN would lead to a wide variety of applications. In fact, it has been well demonstrated that the performance of a graphene device fabricated on a h-BN substrate is much better than that of a conventional device on SiO_2 [4].

Thermal chemical vapor deposition (CVD) is a very powerful technique for large-area thin film growth with a low fabrication cost. Graphene growth by thermal CVD is now intensively studied, aiming at industrial applications of graphene. Thermal CVD growth of h-BN has also been reported in this several decades [5,6]. Even monolayer h-BN has been synthesized by thermal decomposition of borazine ($B_3N_3H_6$) in an ultrahigh vacuum chamber [7]. However, there have only been a few reports on growth of an atomically thin and well-crystallized h-BN film with a conventional CVD apparatus. Song et al. [8] synthesized h-BN films of 2-5 ML on a Cu substrate using ammonia borane (NH_3-BH_3) as a feedstock. Their group also reported CVD growth of h-BN/graphene stacked layers on a Cu substrate [9]. Shi et al. reported growth of $\sim$ 5-50 nm-thick h-BN on a Ni substrate using borazine [10].

In this paper, we report CVD growth of nanometer-thick h-BN films on polycrystalline Ni, Co, and Cu substrates using ammonia borane as a feedstock. Much attention will be focused on the substrate material dependence of the structural properties.

II. EXPERIMENTAL

Ammonia borane was used as a B and N feedstock for the thermal CVD growth. A 300-nm-thick polycrystalline Ni, Co, and Cu films were deposited on a SiO_2/Si wafer by radio-frequency magnetron sputtering and used as substrates. The substrate was inserted into a tube furnace and heated up to a growth temperature of 800-990°C (the temperature was monitored by a thermocouple set just outside the tube) in Ar/H_2 atmosphere. When the temperature reached the growth temperature, the tube was once evacuated, and then ammonia borane vapor was introduced into the tube. The pressure during growth ranged from 50 to 1500 Pa and the growth time was 3 to 30 min. After the growth, the ammonia borane vapor was quickly evacuated and the sample temperature was kept at the growth temperature in Ar atmosphere or a vacuum for $\sim$5 min to avoid possible physisorption of precursor molecules on the sample surface. Then, the sample was cooled down naturally. An optical microscope image of a Ni sample after CVD is shown in Fig. 1. We can clearly observe Ni grains formed at the CVD temperature even after the CVD growth, because the CVD-grown film is highly transparent. The films were grown on such polycrystalline metal film consisting of grains of 1-10 μm scale.

UV-visible light reflectance spectra were obtained using a JASCO V-650 spectrometer. Micro-Raman (Renishaw, Invia) measurements were performed at the excitation wavelength of 532 nm. X-ray photoelectron spectra (XPS) were measured using a monochromatic Al Kα source (1486.6 eV). These measurements were carried out using as-grown films on the metal substrates. For optical

FIG. 1. Optical microscope image of a Ni substrate after CVD growth. Scale bar: 20 μm.

---

microscope and atomic force microscope (AFM) observations, the films were transferred onto a SiO$_2$/Si substrate. Protective poly(methyl methacrylate) (PMMA) film was spin-coated on the h-BN film, and the PMMA/h-BN film was removed from the metal substrate by etching the metal in FeCl$_3$ solution of 1 M. The PMMA/h-BN film was rinsed in deionized water and transferred onto another SiO$_2$/Si substrate. Finally, the PMMA film was removed by either immersion in acetone or heating at 400°C in H$_2$ atmosphere. Similarly, for transmission electron microscopy (TEM) and electron energy loss spectroscopy (EELS) measurements, the h-BN film was transferred onto a TEM grid. The TEM (JEOL JEM-2100F) was operated at 200 kV. For electric measurements, the film was transferred onto a SiO$_2$ (285 nm)/Si (heavily doped) substrate. A field effect transistor device (channel length and width of $\sim 50\,\mu$m and $\sim 2.5\,\mu$m) was fabricated on a SiO$_2$ (285 nm)/Si (heavily doped) substrate using photolithography, oxygen plasma etching, electron beam deposition of Au/Cr electrodes, and lift-off techniques. The substrate worked as a back-gate. Electric measurements were carried out at room temperature in a probing station evacuated by a turbo molecular pump ($\sim 10^{-4}$ Pa).

FIG. 2. (a) Wide-range, (b) B 1s, (c) N 1s, and (d) C 1s XPS of the films grown on Ni, Co, and Cu. In (a), a spectrum of graphene is shown for reference. In (b), (c), and (d) typical binding energy positions are denoted.

III. RESULTS

The compositions of the films were analyzed by core-level XPS. Figure 2(a) shows wide range XPS of films grown on Ni, Co, and Cu substrates and of graphene grown on Ni from spin-coated polyaniline [11] for reference. The B 1s and N 1s peaks are clearly observed from the films. The C 1s signal should be at least partly due to surface contamination, because the samples were exposed to air prior to the measurements. We think that the O 1s signal is mainly due to molecules adsorbed on the surface and edge of the grains and that the O 1s peak intensity would be significantly reduced by annealing in a vacuum, as demonstrated in a previous report [12]. Unfortunately, however, annealing in a vacuum prior to the XPS measurements was not possible due to an apparatus-related restriction of the XPS system. The O 1s peak was also observed for the graphene film. The relative compositions of B, C, and N atoms did not strongly depend on the substrate and were determined to be B$_{0.35}$C$_{0.25}$N$_{0.40}$ (on Ni), B$_{0.38}$C$_{0.22}$N$_{0.40}$ (on Co), and B$_{0.38}$C$_{0.27}$N$_{0.35}$ (on Cu). The B and N contents were approximately the same. The B 1s and N 1s spectra are shown in Figs. 2(b) and (c). Typical binding energy positions [13-17] of some related chemical bonds are denoted in the figures. The B 1s and N 1s peak positions are close to those of h-BN regardless of the substrate, and are observed at around 190.8 and 398.5 eV, respectively. The binding energy difference is about 207.7 eV for all cases, and this value is almost consistent with those of previous reports (207.5-208.0 eV [13, 15-17]). Although the B and N 1s spectra are slightly asymmetric on Co, they show similar shapes. Considering that h-BN has a large band gap, the asymmetry may be attributed to variations of local Fermi energy positions caused by defects or impurities. On Cu, only the B 1s spectrum has a tail at the high binding energy side, and this may be due to an oxide component caused by a small
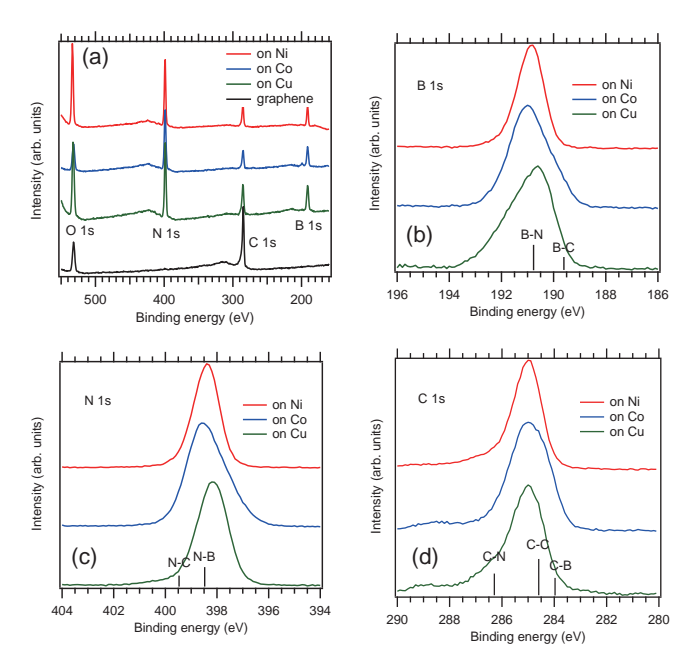
number of excess B atoms. Fig. 2(d) shows the C 1s spectra. On Co, the spectrum is broad, and one may think that there are considerable contributions from C-B and C-N bonds. However, an N-C component is not clearly observed in the N 1s spectrum. On Cu, although the high-binding-energy component looks like a C-N bond, the corresponding component is not clearly observed in the N 1s spectrum, either. We therefore think that there are not large C-B and C-N components and that the C spectra are at least mainly from surface contamination on the grown film. However, we do not fully exclude the possibility that C of several at

Wide-range EEL spectra of films grown on Ni, Co, and Cu are shown in Fig. 3(a). For reference, spectra of h-BN and B$_2$O$_3$ in powder forms are also shown. The B-K, and N-K EELS are commonly observed from the films and the intensity ratio is similar to the reference sample h-BN. Figure 3(b) shows the B-K near-edge structures of the films and reference samples. All the spectra of the films are almost identical to that of h-BN. The peaks at 192 and 200 eV are assigned to $1s \rightarrow \pi^*$ and $1s \rightarrow \sigma^*$ transitions and characteristic of h-BN [18]. A peak at ~ 192 eV is also observed for B$_2$O$_3$; however, the higher energy spectrum is distinctly different from the others. Thus, we did not observe any clear indication of incorporation of B$_2$O$_3$ in the films, including on Cu. The N-K near-edge structures are shown in Fig. 3(c). The transitions to the π^* and σ^* are also observed at ~ 403 and 411 eV, due to hybridization of B and N atomic orbitals in the unoccupied states. All the spectra of the films are consistent with that of h-BN, again.

The existence of a h-BN film on a metal substrate can be easily checked by reflectance spectroscopy in the UV region [19]. The reflectance spectra of films grown on Ni, Co, and Cu are shown in Fig. 4. The spectra at low energies are mainly from the metal substrates under the
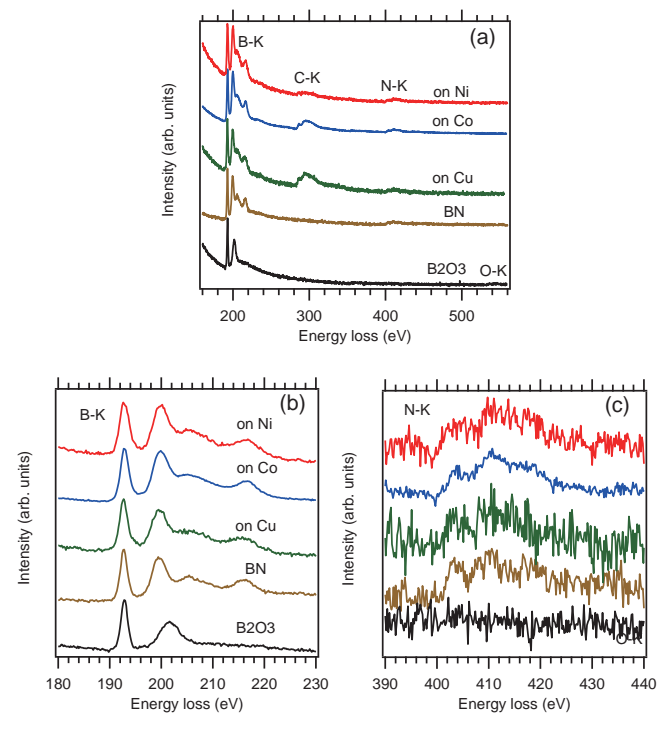
FIG. 3. (a) Wide-range, (b) B-*K*, and (c) N-*K* EELS of films grown on Ni, Co, and Cu. Spectra of BN and B$_2$O$_3$ are also shown for reference.
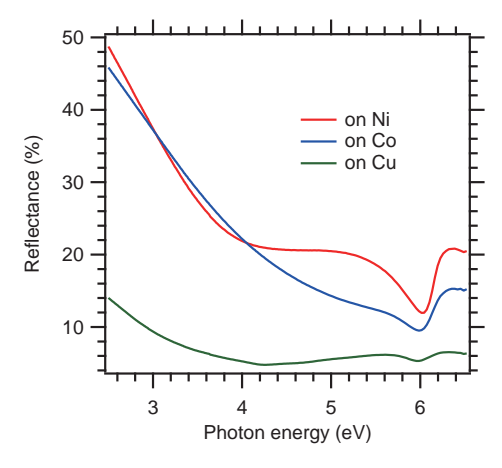

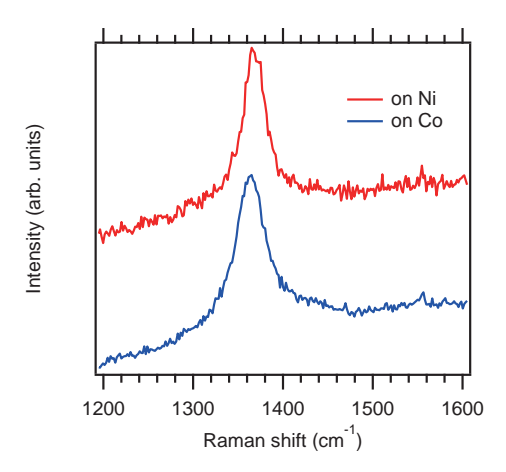FIG. 4. Reflectance spectra of films grown on Ni, Co, and Cu.

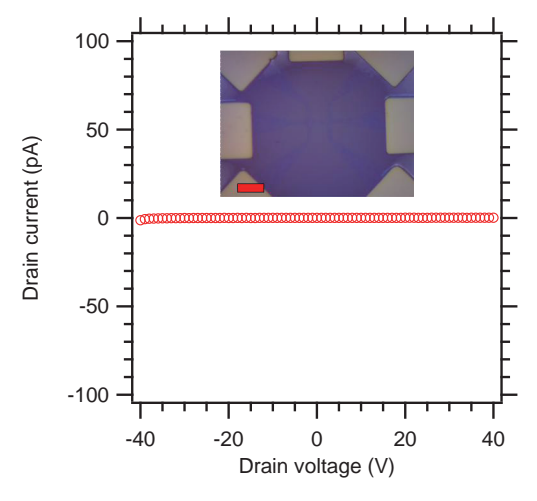FIG. 5. Raman spectra of a film grown on a Ni and Co substrate.

FIG. 6. Current-voltage characteristics of a h-BN device obtained at the gate voltage of 0 V. The inset shows an optical microscope image of the device. Scale bar: 10 μm.

CVD-grown films. The spectra commonly show a peak at 6.3 eV ($\lambda \sim 195$ nm), which is indicative of h-BN [20,21]. The peak height can be an indicator of relative film thickness. The three films were grown under the same conditions (950°C growth temperature, 1000 Pa vapor pressure, 3 min growth time), except for the differences in the substrate materials. The thicknesses on Ni and Co are close, and that on Cu is about one-fifth of those. We will further address this issue below.

The Raman spectra of relatively thick (~ 10 nm or larger) films grown on a Ni and Co substrate are shown in Fig. 5. A single peak was observed at about 1367 cm^{-1}. This peak can be assigned to the E$_{2g}$ tangential mode of h-BN [22] and thus clearly indicates the formation of h-BN. The slight peak shift to the lower wavenumber side observed on Co was due to a laser-induced temperature increase (the laser power density was ~ 10 times larger). The line widths are 28 and 36 cm^{-1} on Ni and

Co, respectively. Although these values are much larger than those of single crystalline h-BN grown by the high-pressure/high-temperature method (9.1 cm^{-1}) [6] and by metalorganic vapor phase exitaxy (~ 13 cm^{-1}) [23], it is comparable to those of BN nanotubes synthesized at relatively low temperatures of 1200 (27 cm^{-1}) and 1050°C (38 cm^{-1}) [24]. No indication of graphene formation ($\sim$1580 cm^{-1}) is seen in Fig. 5. Unfortunately, we have not observed distinct Raman signal from a h-BN film grown on Cu, probably because the thickness is too small (attempts at growing a thick film on Cu often resulted in discretization of the Cu film).

All the spectroscopic results shown in Figs. 2-5 unambiguously show that it is h-BN films that were grown on the metal substrates.

Figure 6 shows the current-voltage characteristics of a device obtained at a back-gate voltage of 0 V. Almost no current is observed despite the large drain voltage of up to ± 40 V. We could not observe any current in a wide gate voltage range of -40 to 40 V. These results show the h-BN film is highly insulating. This is reasonable when we consider that the band gap of h-BN is very large (~ 6 eV). Semiconducting [3] or even metallic [2] nature at an edge of h-BN has been reported theoretically. In fact, edge conduction has been experimentally reported
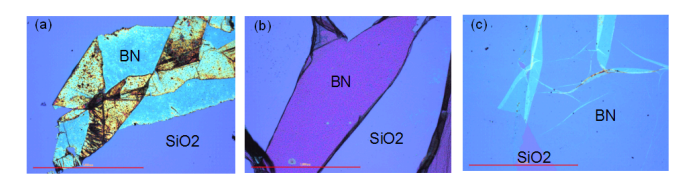
FIG. 7. Low-magnification optical microscope images of BN films grown on (a) Ni, (b), Co, and (c) Cu after transfer onto SiO_2/Si substrates. Scale bars: 1 mm.
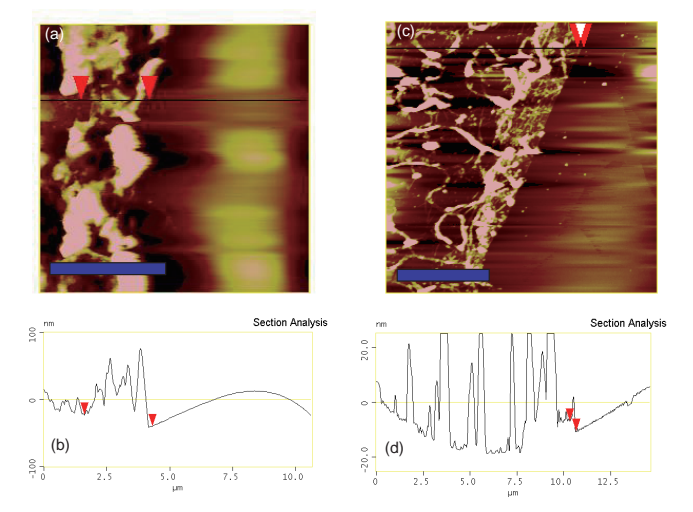

FIG. 8. (a) AFM image of a h-BN film grown on Ni after transfer onto a SiO_2/Si substrate. (b) Height profile along the line in (a). (c) AFM image of a h-BN film grown on Cu after transfer onto a SiO_2/Si substrate. (d) Height profile along the line in (c).
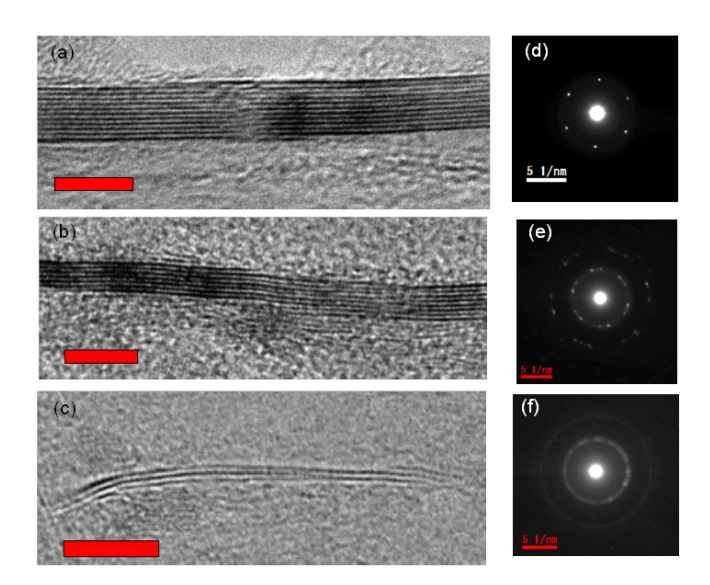

FIG. 9. (a)-(c) TEM image of h-BN films grown on (a) Ni, (b) Co, and (c) Cu. (d)-(f) SAED patterns of h-BN films grown on (d) Ni, (e) Co, and (f) Cu. In (a)-(c), scale bars: 5 nm.

for a BN nanoribbon formed by unwrapping a multiwall BN nanotube [2]. Although the detailed reason for the discrepancy is not clear at present, it may originate in the differences in the detailed edge structures. Our result is consistent with a previous report in which no conduction was observed from a CVD-grown h-BN film [8].

Hereafter, we mainly focus on the structural properties and their substrate material dependence. Low-magnification optical microscope images of h-BN films after the films had been transferred onto SiO_2 (285 nm)/Si substrates are shown in Fig. 7. The relatively thick films were intentionally grown on (a) Ni, (b) Co, and (c) Cu at the same conditions (950°C, 1500 Pa, 30 min). The observed folding, rolling, and corrugation were formed during the transfer process. The film grown on Cu shows weaker contrast, indicating that it is thinner. AFM images and height profiles obtained from the h-BN films shown in Figs. 7(a) and (c) are shown in Fig. 8. The ribbon-like feature seen in Fig. 8(c) is corrugation formed around holes in the Cu film (at a high temperature, holes are often formed in Cu films). Although precise height determination was difficult due to the corrugation of the transferred film, the thickness of the film grown on Ni was estimated to be ~ 20 nm or larger and that the film grown on Cu to be ~ 4 nm. These results show that the film thickness strongly depends on the substrate material and that a thinner film is obtained on Cu. They are consistent with the reflection spectroscopy results shown in Fig. 4.

Cross-sectional TEM images of films grown on (a) Ni, (b) Co, and (c) Cu are shown in Fig. 9. These images were obtained from corrugated parts of the films. Layered structures are clearly observed for all the substrates. The layer-repeat distance was evaluated to be 0.33 ± 0.03 nm, which is consistent with that of h-BN (0.333 nm [25]). The films grown on Ni and Co were obtained at the same growth condition (900°C, 70 Pa, 7 min). About 12 and 8 layers are seen in Figs. 9(a) and (b). The numbers of layers observed from the films ranged from 7 to 12 and 5 to 8 for Ni and Co, respectively. The average thickness on Co is close to or slightly smaller than that on Ni. We can also grow few-layer film as shown in Fig. 9(c). We observed 2 to 6 layers from the film. In this case, the substrate was Cu and growth conditions were 990°C, 1000 Pa, and 3 min. Reflection spectra (not shown, but similar to those in Fig. 4) revealed that thicker films were grown for Ni and Co again under this condition.

We also found that the stacking or domain structure depends on the substrate material. Selected area (~ 150 nm) electron diffraction patterns obtained from the films in Fig. 9(a)-(c) are shown in Figs. 9(d)-(f). Six-fold symmetry is observed for all substrates. A single set of spots was often observed from the film grown on Ni, as shown in Fig. 9(d), although the number of layers is the largest. This indicates that the layers are stacked quite regularly. We can expect that B and N atoms are aligned alternately in the c direction, as in bulk h-BN [25]. A few sets of spots were observed from the film grown on Co. Despite its having the smallest number of layers, the film grown on Cu shows a ring-like pattern, indicating that the stacking is highly turbostratic or the film consists of domains much smaller than the beam size of 150 nm. Thus, stacking disorder increases or domain size decreases in the order of a Ni, Co, and Cu substrate.

IV.   DISCUSSION

As shown above, substrate material dependence of film thickness and stacking/domain structure was observed for Ni, Co, and Cu. A smaller thickness and more turbostratic stacking/smaller domains were observed for a Cu substrate than for Ni and Co substrates at the same growth condition. Similarly, a thick (up to ~ 50 nm) and regularly stacked film on Ni [10] and a thin (2-5 ML) and turbostratically stacked film on Cu [8] were also observed in previous studies on the CVD growth of h-BN, although feedstocks used in the two studies were different. These strongly suggest that the substrate has an essentially important role for the CVD growth of a h-BN film. The metal surface has a catalytic function for decomposition of the feedstock molecule and the degree of the catalytic function would depend on the material. However, the differences in the catalytic function do not explain the results because the metal surface was entirely covered by few-layer or multilayer h-BN regardless of the substrate material in this study. Similar substrate dependence of thickness and stacking structure have been observed for growth of graphene on a metal substrate. On Ni, a larger thickness and more regular stacking have been observed [26,27], whereas a smaller thickness and turbostratic stacking have been observed on a Cu substrate [28]. In the case of graphene, the substrate dependence has been considered to be due to differences in carbon solubility and to consequent different growth mechanisms. On Ni, which has high carbon solubility at growth temperatures (~ 0.9 at.% at 900°C), graphene growth by CVD occurs mainly by segregation or precipitation during cooling [29]. This tends to result in the growth of thick graphene film and probably regular stacking. On the other hand, a graphene film is grown by surface absorption on Cu [27], which has a much lower carbon solubility (~ 0.005-0.04 at.% at 1084°C [30]). Consequently, a thinner and turbostratic stacked film is formed. Growth of h-BN on Cu may also be dominated by surface adsorption. However, in the case of h-BN growth on Ni, it does not seem that the above scenario can simply be applied. Although Ni has a considerably high B solubility (0.3 % at 1085°C [31]), N solubility has been reported to be almost zero in molten Ni [31] and ~ 0.005 at.% even

at an extremely high temperature of 1600°C [32]. At this stage, the concrete reason for the substrate dependence is unclear. However, the substrate dependence similar to that in graphene growth suggests that the substrate plays an important role for providing the surface with B and N atoms at least at the initial stage of the CVD growth. One possibility may be that B and N atoms are accommodated in the grain boundaries of polycrystalline Ni and Co substrates at the CVD temperatures, and they segregate and form h-BN at lower temperatures. In fact, CVD growth of graphene at a Cu/SiO$_2$ interface through the Cu film has been reported [33]. In this case, carbon atoms are believed to diffuse from the Cu surface to the Cu/SiO$_2$ interface through grain boundaries.

V.   CONCLUSIONS

Nanometer-thick thin films were grown on Ni, Co, and Cu substrates by thermal CVD using ammonia borane as a feedstock. XPS, EELS, reflection spectroscopy, Raman spectroscopy, and TEM observation revealed that h-BN is grown regardless of the substrate. A thicker and thinner film was grown on Ni and Cu. More regular stacking was observed on Ni and more turbostratic or smaller domain size was observed on Cu. This substrate dependence is basically similar to that observed in graphene growth, and suggests an important role of the substrate for h-BN growth. However, the segregation or precipitation mechanism proposed for graphene growth on Ni can not be simply applied to h-BN growth, because nitrogen is almost insoluble in Ni. We think that B and N atoms are accommodated at the grain boundaries of the polycrystalline metal substrates.

[1] K. Watanabe, T. Taniguchi, and H. Kanda, Nature Mater. **3**, 404 (2004).

[2] H. Zeng, C. Zhi, Z. Zhang, X. Wei, X. Wang, W. Guo, Y. Bando, and D. Golberg, Nano. Lett. **10**, 5049 (2010).

[3] Y. Liu, S. Bhowmick, and B. I. Yakobson, Nano. Lett. **11**, 3113 (2011).

[4] C. R. Dean, A. F. Young, I. Meric, C. Lee, L. Wang, S. Sorgenfrei, K. Watanabe, T. Taniguchi, P. Kim, K. L. Shepard, and J. Hone, Nature Nanotechnol. **5**, 722 (2010).

[5] M. Rand and J. Roberts, J. Electrochem. Soc. **115**, 423 (1968), and references therein.

[6] O. Tsuda, K. Watanabe, and T. Taniguchi, Jpn. J. Appl. Phys. **46**, L287 (2007).

[7] A. Nagashima, N. Tejima, Y. Gamou, T. Kawai, and C. Oshima, Surf. Sci. **357-358**, 307 (1996).

[8] L. Song, L. Ci, H. Lu, P. B. Sorokin, C. Jin, J. Ni, A. G. Kvashnin, D. G. Kvashnin, J. Lou, B. I. Yakobson, and P. M. Ajayan, Nano Lett. **10**, 3209 (2010).

[9] Z. Liu, L. Song, S. Zhao, J. Huang, L. Ma, J. Zhang, J. Lou, and P. M. Ajayan, Nano Lett. **11**, 2032 (2011).

[10] Y. Shi, C. Hamsen, X. Jia, K. Kim, A. Reina, M. Hofmann, A. L. Hsu, K. Zhang, H. Li, Z. Juang, M. S. Dresselhaus, L. Li, and J. Kong, Nano Lett. **10**, 4134 (2010).

[11] S. Suzuki, Y. Takei, K. Furukawa, G. Webber, S. Tanabe, and H. Hibino, Jpn. J. Appl. Phys. **50** (2012), in press.

[12] D. Wei, Y. Liu, Y. Wang, H. Zhang, L. Huang, and G. Yu, Nano Lett. **9**, 1752 (2009).

[13] M.O. Watanabe, S. Itoh, K. Mizushima, and T. Sasaki, Appl. Phys. Lett. **68**, 2962 (1996).

[14] M. A. Mannnan, Y. Baba, T. Kida, M. Nagano, I. Shimoyama, N. Hirao, and H. Noguchi, Thin Solid Films **519**,

1780 (2011).

[15] S. Nakao, T. Sonoda, K. Tsugawa, J. Choi, and T. Kato, Vacuum **84**, 642 (2009).

[16] E. Bengu, M.F. Genisel, O. Gulseren, and R. Ovali, Thin Solid Films **518**, 1459 (2009).

[17] S. Kim, J. Park, H. Choi, J. Ahn, J. Hou, and J. Kang, J. Am. Chem. Soc. **129**, 1705 (2007).

[18] A. B. Preobrajenski, A. S. Vinogardov, and N. Martensson, Surf. Sci. **582**, 21 (2005).

[19] S. Suzuki and H. Hibino, Mater. Sci. Eng. B **177**, 233 (2012).

[20] D. M. Hoffman, G. L. Doll, and P. C. Eklund, Phys. Rev. B **30**, 6051 (1984).

[21] A. Chayahara, H. Yokoyama, T. Imura, Y. Osaka, and M. Fujisawa, Jpn. J. Appl. Phys. **27**, 440 (1988).

[22] S. Reich, A. C. Ferrari, R. Arenal, A. Loiseau, I. Bello, and J. Robsrtson, Phys. Rev. B **71**, 205201 (2005).

[23] Y. Kobayashi and T. Akasaka, J. Cryst. Growth **310**, 5044 (2008).

[24] S. Bae, H. Seo, J. Park, Y. Choi, J. Park, and S. Lee, Chem. Phys. Lett. **374**, 534 (2003).

[25] D. Golberg, Y. Bando, Y. Huang, T. Terao, M. Mitome, C. Tang, and C. Zhi, ACS Nano **4**, 2979 (2010).

[26] A. Johansson, J. Lu, and J. Carlsson, Thin Solid Films **252**, 19 (1994).

[27] A. Reina, X. Jia, J. Ho, D. Nezich, H. Son, V. Bulovic, M. S. Dresselhaus, and J. Kong, Nano Lett. **9**, 30 (2009).

[28] T. P. Ong, F. Xiong, R. P. H. Chang, and C. W. J. White, J. Mater. Res. **7**, 2429 (1992).

[29] X. Li, W. Cai, L. Colombo, and R. S. Ruoff, Nano Lett. **9**, 4268 (2009).

[30] C. Mattevi, H. Kim, and M. Chhowalla, J. Mater. Chem. **21**, 3324 (2011).

[31] P. C. Yang, J. T. Prater, W. Liu, J. T. Glass, and R. F. Davis, J. Electronic Mater. **34**, 1558 (2005).

[32] M. Kawasaki, M. Tokuda, and M. Ohtani, Tohoku Daigaku Senko Seiren Kenkyujo Ihou **35**, 99 (1980) [in Japanese].

[33] C. Su, A. Lu, C. Wu Y. Li, K. Liu, W. Zhang, S. Lin, Z. Juang, Y. Zhong, F. Chen, and L. Li, Nano Lett. **11**, 3612 (2011).